Supporting Information

Mediated Water Electrolysis in Biphasic Systems

Micheál D. Scanlon,[a,*] Pekka Peljo,[b] Lucie Rivier,[b] Heron Vrubel[b] and Hubert H. Girault[b,*]

[a] *The Bernal Institute and Department of Chemical Sciences, School of Natural Sciences, University of Limerick (UL), Limerick V94 T9PX, Ireland.*

[b] *Laboratoire d'Electrochimie Physique et Analytique (LEPA), Ecole Polytechnique Fédérale de Lausanne (EPFL) Rue de l'Industrie 17, CH-1951 Sion, Switzerland.*

**Corresponding authors.*

E-mail addresses: micheal.scanlon@ul.ie (M.D. Scanlon), hubert.girault@epfl.ch (H.H. Girault)

ESI-1: Experimental methods.

1.1 Synthetic procedures

A dry powder of the strong organic tetrakis(pentafluorophenyl)borate diethyl etherate acid ([$H(OEt_2)_2$]TB) was prepared as follows. Briefly, 2 g of [$Li(OEt_2)_2$]TB was dissolved in 30 mL of 6 M HCl to prepare [$H(OEt_2)_2$]TB. To ensure that the di-solvated $H(OEt_2)_2^+$ cation was formed a few millilitres of diethyl ether were added to this mixture. The latter is a critical step in the synthesis as the non-etherated version of this acid, [H]TB, although predicted to be an exceptionally strong acid,[1] cannot be synthesised as the TB^- anion is unstable with respect to B-phenyl bond cleavage.[2] The diethyl etherate prepared here is a weaker acid than the theoretical non-etherated [H]TB but much more stable.[3–5] Next, [$H(OEt_2)_2$]TB was extracted by addition of DCM (30 mL) and the aqueous layer was further washed with DCM (2 × 15 mL) after phase separation. The combined organic layers were dried over Na_2SO_4. Finally, Na_2SO_4 was removed by filtration and DCM evaporated under reduced pressure to yield the organic soluble acid [$H(OEt_2)_2$]TB as a white powder.

The synthesis of [$Cp^*_2Fe^{(III)}$]TB was carried out by oxidation of $Cp^*_2Fe^{(II)}$ with [$H(OEt_2)_2$]TB in dry DCM. Therefore, [$H(OEt_2)_2$]TB was firstly prepared in DCM as described *vide supra*, but the DCM was not evaporated under reduced pressure. Thus, initially [$Li(OEt_2)_2$]TB was dissolved in 30 mL of water. To this viscous solution, 30 mL of 12 M HCl were added. An organic phase separates upon the addition of acid. The mixture was allowed to cool down to ambient temperature and 5 mL of Et_2O was added to help the formation of the $[H(OEt_2)_2]^+$ cation. The mixture was extracted three times with 50 mL of DCM. The organic phase was dried with anhydrous Na_2SO_4 and filtered. The Na_2SO_4 cake was washed twice with 20 mL of DCM to extract all [$H(OEt_2)_2$]TB.

1.70 g (5.21 mmol) of solid $Cp^*_2Fe^{(II)}$ was added to the DCM solution with immediate formation of the green color of $[Cp^*_2Fe^{(III)}]^+$. The solution was left stirring for 1 hour to ensure the complete oxidation of $Cp^*_2Fe^{(II)}$. The volume of the solution was reduced to *ca.* 25mL in a rotary evaporator. 150 mL of Et_2O was added to the solution which was kept in the freezer (-18 °C) overnight. The green crystals of [$Cp^*_2Fe^{(III)}$]TB were collected by filtration, washed with cold Et_2O and dried under vacuum. The yield was 4.5g (86%).

1.2 Construction of a Double-Juntcion Organic Reference Electrode (DJ-ORE)

To construct the DJ-ORE, a silver wire was soldered to a brass contact (made in a mechanical workshop) and placed in an inner glass chamber containing 10 mM $AgNO_3$ and 100 mM $TBAPF_6$ dissolved in acetonitrile as the filling solution. The inner and outer chambers were connected by a silica gel bead that was fixed to the tip of the glass tube using a transparent heat-shrink fluorinated ethylene propylene tubing (FEP, from Zeus Inc.) by lightly heating with a heat gun. The FEP tubing was specifically chosen due to its superb resistance to organic solvents. The filling solution in the outer chamber contained 100 mM $TBAPF_6$ in acetonitrile, and the latter was connected to the test solution by a cracked-Pt junction.[6,7] The cracked-Pt junction forms an imperfect seal between the platinum wire and the glass body of the DJ-ORE. This serves as a leak through which the filling solution can interact with the electrolyte of the electrochemical cell.

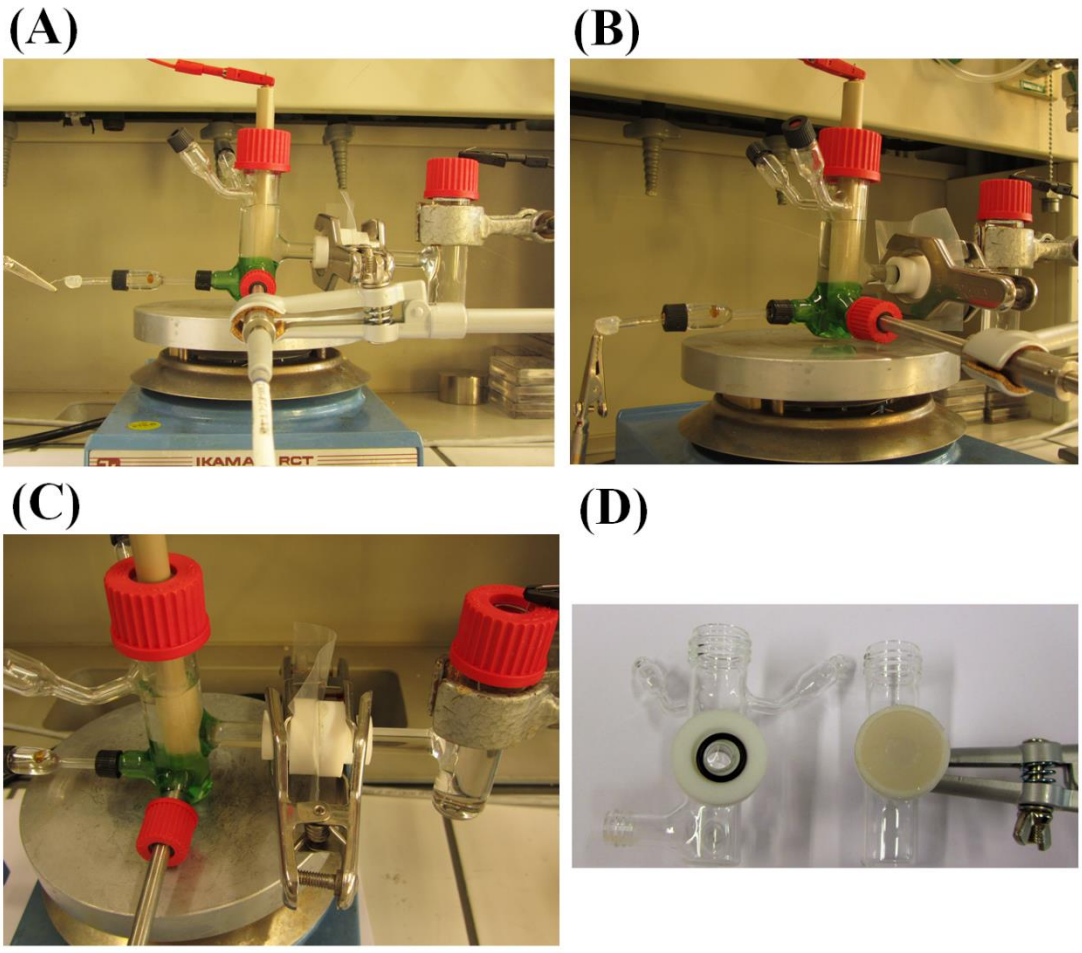

Fig. S1. Images of the biphasic electrolysis H-cell. The individual parts of the H-cell are labelled in Fig. 1, main text.

<u>ESI-2:</u> Spontaneous *versus* photo-induced H_2 evolution at polarized water-organic interfaces with metallocenes.

The Girault Group has pioneered a biphasic approach to the HER. The set-up consists of an organic solution of low water miscibility, typically 1,2-dichloroethane (DCE), containing a dissolved lipophilic electron donor, *e.g.*, a metallocene, that is contacted with an acidic aqueous electrolyte solution. Upon polarization of the resulting water-oil or "soft" interface, either *via* the application of an external voltage or by dissolving a common ion in both phases, protons are pumped into the organic phase and reduced to H_2 by the metallocene (see Schemes 2 and 3 in the main text for more details of the precise mechanism).

The formal reduction potentials for a series of metallocenes in a DCE organic phase ($[E^{0'}_{(ox/red)}]^{DCE}$), *versus* the Standard Hydrogen Electrode (SHE) and *versus* the formal reduction potential of the ferrocenium cation/ferrocene ($[Cp_2Fe^{(III)}]^+/Cp_2Fe^{(II)}$) redox couple in DCE, are summarized in Table 1 (main text). The formal reduction potential of a proton in a DCE organic phase ($[E^{0'}_{(H^+/1/2H_2)}]^{DCE}$) is 0.58 V *vs.* SHE.[8] Thus, thermodynamically, a proton dissolved in DCE is far easier to reduce (*i.e.*, has a more positive standard reduction potential) to H_2 than an aqueous solubilized proton (by definition $[E^{0'}_{(H^+/1/2H_2)}]^{W} = 0$ V *vs.* SHE). The thermodynamic origin for the absolute standard reduction potential of a proton in DCE has been outlined previously.[9,10]

Consequently, organic solubilized protons can be reduced by relatively weak lipophilic electrons donors, with formal reduction potentials more positive than 0 V *vs.* SHE (meaning the electron donors are incapable of directly reducing aqueous protons). Decamethylferrocene ($Cp^*_2Fe^{(II)}$, Cp* = C_5Me_5) has a formal reduction potential over 0.5 V more negative than $[E^{0'}_{(H^+/1/2H_2)}]^{DCE}$. Therefore, when protons are pumped from water into DCE (by polarizing the water-organic interface positively) with $Cp^*_2Fe^{(II)}$ present, H_2 is evolved spontaneously *via* a mechanism that involves the transient formation of the decamethylferrocene hydride species ($[Cp^*_2Fe^{(IV)}(H)]^+$), see Scheme 3 (main text). Heavy metal containing metallocenes such as osmocene ($Cp_2Os^{(II)}$; Cp = C_5H_5), decamethylosmocene ($Cp^*_2Os^{(II)}$) and decamethylruthenocene ($Cp^*_2Ru^{(II)}$) are all much weaker reductants than $Cp^*_2Fe^{(II)}$. Accordingly, none of these metallocenes are capable of reducing protons pumped into DCE spontaneously but, interestingly, all are capable

of evolving H_2 to varying degrees when photo-activated, again *via* the corresponding hydride species, see Scheme 2 (main text). Substantial quantities of H_2 are evolved with $Cp^*_2Os^{(II)}$ and $Cp^*_2Ru^{(II)}$, while $Cp_2Os^{(II)}$, the weakest electron donor, produces only small quantities. As discussed in detail in the main text, the ability to generate H_2 with very weak reductants such as $Cp^*_2Ru^{(II)}$ is ideal for integration into the cathodic compartment of a biphasic H-cell as the oxidized form can be reduced at very positive redox potentials, thereby required less electrochemical driving force (*i.e.*, providing a more efficient use of the renewable electricity supply).

ESI-3: Determining the appropriate potential to apply during biphasic electrolysis to ensure that the metallocene is recycled but H_2 is not evolved directly at the electrode surface.

The reduction of $[Cp_2Fe^{(III)}]^+$ in the presence of organic solubilized protons was investigated by cyclic voltammetry (CV). Three different electrochemical cell configurations were investigated with different combinations of the organic electrolyte salt (100 mM THxABF$_4$ *versus* 100 mM BATB) and the choice of organic acid (so called "dry" *versus* "wet" $H(OEt_2)_2TB$). Thus, the influence of the organic electrolyte salt on the onset potential of H_2 evolution at the glassy carbon electrode was investigated, as was the "nature" of the organic proton.

"Dry" $H(OEt_2)_2TB$ was synthesized as a pure powder, as discussed in section ESI-1.1, and dissolved directly into the DCE. Alternatively, "wet" $H(OEt_2)_2TB$ was extracted into the DCE phase using a shake-flask methodology.[11] Briefly, the shake-flask approach involved contacting an aqueous phase containing *x* mM $Li(OEt_2)_2TB$ and 100 mM HCl with an identical volume of DCE containing *y* mM $[Cp_2*Fe^{(III)}]TB$ and 100 mM BATB. After stirring for 2 hours, *x* mM of "wet" $H(OEt_2)_2TB$ was extracted to the DCE phase and the aqueous phase was discarded. Proton extraction occurs as an interfacial Galvani potential difference ($\Delta_o^w\phi$) was established due to the distribution of lipophilic TB^- anions. Consequently, with TB^- acting as a phase transfer catalyst, etherated protons ($H(OEt_2)_2^+$) were extracted or "pumped" to DCE almost quantitatively as $H(OEt_2)_2TB$. "Wet" $H(OEt_2)_2TB$ represents most closely the form of the proton transferred from the water to organic phase during biphasic electrolysis. Thus, the three DCE phases studied contained:

(i) *x* mM "dry" $H(OEt_2)_2TB$, *y* mM $[Cp_2Fe^{(III)}]TB$ and 100 mM THxABF$_4$

(ii) *x* mM "dry" $H(OEt_2)_2TB$, *y* mM $[Cp_2Fe^{(III)}]TB$ and 100 mM BATB

(iii) *x* mM "wet" $H(OEt_2)_2TB$, *y* mM $[Cp_2Fe^{(III)}]TB$ and 100 mM BATB

Cyclic voltammograms (CVs) for each electrochemical cell are shown in Fig. S2 and obtained as described in the Electrochemical Measurements section of the main text. A summary of the H_2 evolution onset potentials in the presence of $[Cp_2Fe^{(III)}]TB$ for each electrochemical cell is presented in Table S1.

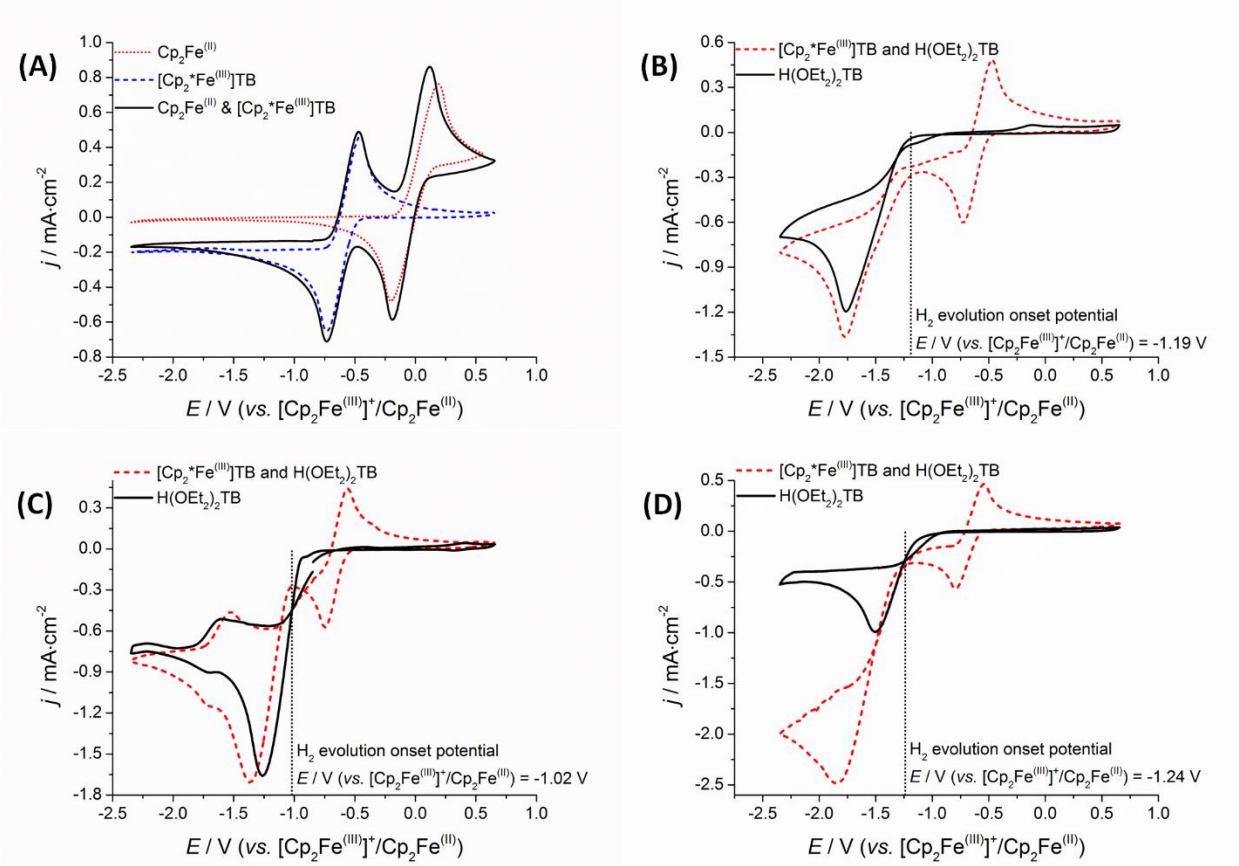

Fig. S2. Determining the correct potential to apply during chronoamperometry to facilitate $[Cp_2Fe^{(III)}]^+$ reduction but prevent direct H_2 evolution at the glassy carbon electrode surface. **(A)** All cyclic voltammograms (CVs) were calibrated *versus* the $Cp_2Fe^{(III)}]^+/Cp_2Fe^{(II)}$ redox couple as highlighted by comparison of the CVs of $Cp_2Fe^{(II)}$ (5 mM, red dotted line), $[Cp_2Fe^{(III)}]^+$ (5 mM, blue dashed line), and a mixture of $Cp_2Fe^{(II)}$ and $[Cp_2Fe^{(III)}]^+$ (both 5 mM, solid black line), respectively, in DCE containing 100 mM BATB organic electrolyte salt. Organic proton reduction both in the presence (red dashed lines) and absence (solid black line) of $[Cp_2Fe^{(III)}]^+$ for electrochemical cells **(B)** with synthesized "dry" $H(OEt_2)_2TB$ (20 mM) as the organic proton source and 100 mM $THxABF_4$ as the organic electrolyte salt, **(C)** with synthesized "dry" $H(OEt_2)_2TB$ (20 mM) and 100 mM BATB, and **(D)** with "wet" $H(OEt_2)_2TB$ (30 mM in the presence and 17 mM in the absence of $[Cp_2Fe^{(III)}]^+$) extracted from an acidic aqueous phase using a shake-flask approach and 100 mM BATB. All CVs were obtained under anaerobic conditions, using degassed DCE solutions, in a glovebox and at a scan rate of 50 $mV \cdot s^{-1}$.

Table S1: H_2 evolution onset potentials in the presence of $[Cp_2Fe^{(III)}]TB$ at a glassy carbon electrode immersed in degassed DCE solutions. The onset potentials, measured *vs.* a Ag^+/Ag double-junction organic reference electrode, were calibrated *vs.* the $[Cp_2Fe^{(III)}]^+/Cp_2Fe^{(II)}$ redox couple. Furthermore, the onset potentials can be expressed on the standard hydrogen electrode (SHE) scale as the formal redox potential of $Cp_2Fe^{(II)}$ in DCE ($[E^{0\prime}_{([Cp_2Fe^{(III)}]^+/Cp_2Fe^{(II)})}]^{DCE}$) has been determined previously as 0.640 V *vs.* SHE from cyclic voltammetry experiments at polarized water-DCE interfaces and verified by evaluating thermodynamic cycles.[12]

Electrochemical cell	**H_2 evolution onset potentials**		
	E **(V *vs.* Ag^+/Ag)**	***E*** **(V *vs.* $[Cp_2Fe^{(III)}]^+/Cp_2Fe^{(II)}$)**	***E*** **(V *vs.* SHE)**
"dry" $H(OEt_2)_2TB$/ $THxABF_4$	–0.826	–1.190	–0.550
"dry" $H(OEt_2)_2TB$/BATB	–0.656	–1.020	–0.380
"wet" $H(OEt_2)_2TB$/BATB	–0.876	–1.240	–0.600

The onset potential for H_2 decreased slightly by 50 mV with $THxABF_4$ organic electrolyte in comparison to BATB with "wet" $H(OEt_2)_2TB$. However, a major shift was noted between the two methods of preparing the etherated organic soluble protons. The so-called "dry" $H(OEt_2)_2TB$ dramatically decreased the onset potential by 220 mV in comparison to the "wet" $H(OEt_2)_2TB$, extracted into DCE using the shake-flask methodology. The precise reasons for this large change in H_2 evolution onset potential are outside the scope of the present study. However, speculatively, perhaps the wet" $H(OEt_2)_2TB$ has an associated solvation-shell not present for the directly synthesized "dry" $H(OEt_2)_2TB$ species. This solvation shell may hamper the interaction of the $H(OEt_2)_2TB$ molecule with the glassy carbon electrode, increasing the H_2 evolution onset potential.

As the "wet" $H(OEt_2)_2TB$ most closely represents the form of the proton encountered by the glassy carbon electrode during biphasic electrolysis, **a potential of –1.164 V *vs.* $[Cp_2Fe^{(III)}]^+/Cp_2Fe^{(II)}$ (or –0.524 V vs. SHE) was applied for all biphasic electrolysis experiments.** This potential is sufficient to drive the reduction of $[Cp_2Fe^{(III)}]^+$ at an appreciable rate (since $[E^{0\prime}_{([Cp_2Fe^{(III)}]^+/Cp_2Fe^{(II)})}]^{DCE} = -0.600$ V vs. $[Cp_2Fe^{(III)}]^+/Cp_2Fe^{(II)}$, see Table 1, main text), while avoiding direct H_2 evolution in the presence of either $THxABF_4$ or BATB organic electrolyte.

ESI-4: Gas chromatography studies of H_2 evolved during biphasic electrolysis.

Gas chromatography (GC) measurements were carried out post-biphasic electrolysis. The GC measurements are qualitative as H_2 is an extremely "leaky" molecule. It is known that H_2 can diffuse through a Nafion® membrane.[13,14] Therefore, even though the cathodic compartment was completely sealed, it is possible that over the 22 hour period H_2 was escaping through the Nafion® membrane. Nevertheless, greater quantities of H_2 were consistently detected for biphasic electrolysis experiments with the Mo_2C H_2 evolution catalyst floating at the water-organic interface (so biphasic electrolysis cell 3, described in Schemes 4 and 5, main text).

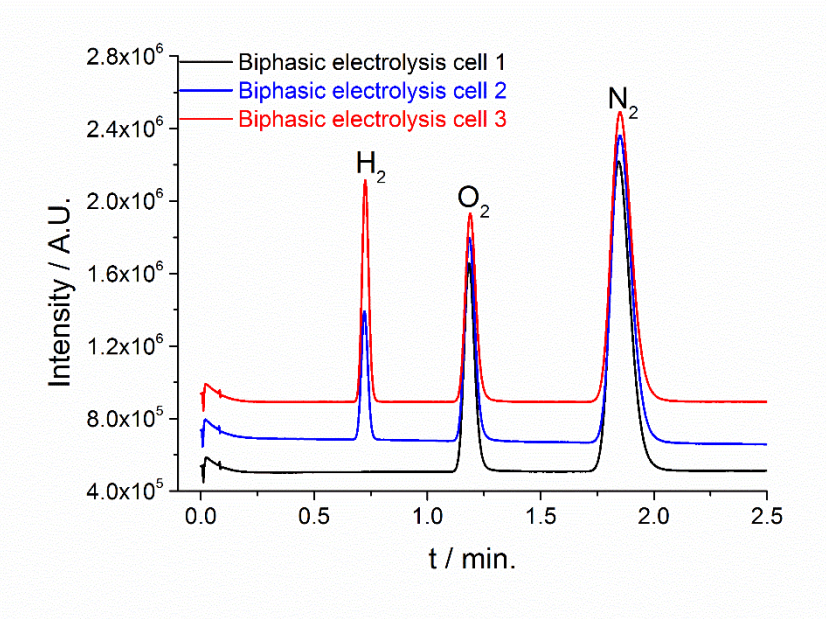

Fig S3. Gas chromatograms (GC) of the headspace in the working electrode compartment after 22 hours of biphasic electrolysis for the three biphasic electrochemical cell configurations described in Schemes 4 and 5, main text. The GC data provided a qualitative indication that H_2 is only formed during biphasic electrolysis experiments with BATB as the organic electrolyte salt.

Supplementary references

1 E. S. Stoyanov, K. C. Kim and C. A. Reed, *J. Am. Chem. Soc.*, 2006, **128**, 8500–8508.

2 C. A. Reed, K. C. Kim, E. S. Stoyanov, D. Stasko, F. S. Tham, L. J. Mueller and P. D. W. Boyd, *J. Am. Chem. Soc.*, 2003, **125**, 1796–1804.

3 P. Jutzi, C. Müller, A. Stammler and H. Stammler, *Organometallics*, 2000, **19**, 1442–1444.

4 C. A. Reed, *Acc. Chem. Res.*, 2010, **43**, 121–128.

5 C. A. Reed, *Acc. Chem. Res.*, 2013, **46**, 2567–2575.

6 D. T. Sawyer, A. J. Sobkowiak and J. Roberts, Jr., in *Electrochemistry for Chemists*, John Wiley & Sons, Ltd, New York, 2nd edn., 1995, pp. 170–248.

7 T. J. Smith and K. J. Stevenson, in *Handbook of Electrochemistry*, ed. C. J. Zoski, Elsevier B.V, 2007, pp. 73–110.

8 A. J. Olaya, M. A. Méndez, F. Cortes-Salazar and H. H. Girault, *J. Electroanal. Chem.*, 2010, **644**, 60–66.

9 H. H. Girault, *Analytical and Physical Electrochemistry*, EPFL Press, 2004.

10 I. Hatay, B. Su, F. Li, R. Partovi-Nia, H. Vrubel, X. Hu, M. Ersoz and H. H. Girault, *Angew. Chemie - Int. Ed.*, 2009, **48**, 5139–5142.

11 X. Bian, M. D. Scanlon, S. Wang, L. Liao, Y. Tang, B. Liu and H. H. Girault, *Chem. Sci.*, 2013, **4**, 3432–3441.

12 D. J. Fermin and R. Lahtinen, in *Liquid Interfaces In Chemical, Biological And Pharmaceutical Applications*, ed. A. G. Volkov, CRC Press, 2001, pp. 179–228.

13 M. Schalenbach, T. Hoefner, P. Paciok, M. Carmo, W. Lueke and D. Stolten, *J. Phys. Chem. C*, 2015, **119**, 25145–25155.

14 K. Broka and P. Ekdunge, *J. Appl. Electrochem.*, 1997, **27**, 117–123.